

AD-A076 109

ARMY ENGINEER TOPOGRAPHIC LABS FORT BELVOIR VA
FOURIER TRANSFORM AUTOCORRELATION.(U)

F/G 14/5

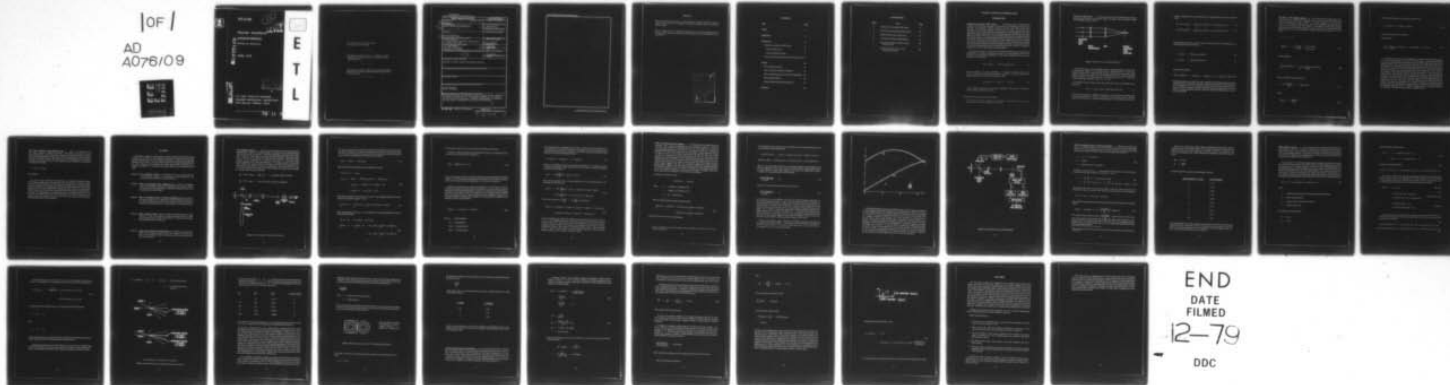
UNCLASSIFIED

APR 79 M M MCDONNELL
ETL-0184

NL

10F /
AD
A076/09

ETL



END
DATE
FILMED
12-79
DDC

ETL-0184

12

LEVEL

**Fourier transform
autocorrelation**

Michael M. McDonnell

APRIL 1979

AD A 076109

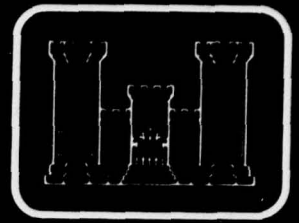
DDC FILE COPY

DDC
RECEIVED
NOV 5 1979
A

U.S. ARMY CORPS OF ENGINEERS
ENGINEER TOPOGRAPHIC LABORATORIES
FORT BELVOIR, VIRGINIA 22060

APPROVED FOR PUBLIC RELEASE; DISTRIBUTION UNLIMITED

79 11 0



E
T
L

Destroy this report when no longer needed.
Do not return it to the originator.

The findings in this report are not to be construed as an official
Department of the Army position unless so designated by other
authorized documents.

The citation in this report of trade names of commercially available
products does not constitute official endorsement or approval of the
use of such products.

UNCLASSIFIED

SECURITY CLASSIFICATION OF THIS PAGE (When Data Entered)

REPORT DOCUMENTATION PAGE		READ INSTRUCTIONS BEFORE COMPLETING FORM
1. REPORT NUMBER ETL-0184	2. GOVT ACCESSION NO.	3. RECIPIENT'S CATALOG NUMBER
4. TITLE (and Subtitle) FOURIER TRANSFORM AUTOCORRELATION.	5. TYPE OF REPORT & PERIOD COVERED Research Note	6. PERFORMING ORG. REPORT NUMBER
7. AUTHOR(s) Michael M. McDonnell	8. CONTRACT OR GRANT NUMBER(s)	
9. PERFORMING ORGANIZATION NAME AND ADDRESS Research Institute U. S. Army Engineer Topographic Laboratories Fort Belvoir, VA 22060	10. PROGRAM ELEMENT, PROJECT, TASK AREA & WORK UNIT NUMBERS 4A161101A91D	
11. CONTROLLING OFFICE NAME AND ADDRESS U. S. Army Engineer Topographic Laboratories Fort Belvoir, VA 22060	12. REPORT DATE Apr 11 1979	13. NUMBER OF PAGES 33
14. MONITORING AGENCY NAME & ADDRESS (if different from Controlling Office) 1236	15. SECURITY CLASS. (of this report) Unclassified	15a. DECLASSIFICATION/DOWNGRADING SCHEDULE
16. DISTRIBUTION STATEMENT (of this Report) Approved for public release; distribution unlimited.		
17. DISTRIBUTION STATEMENT (of the abstract entered in Block 20, if different from Report)		
18. SUPPLEMENTARY NOTES		
19. KEY WORDS (Continue on reverse side if necessary and identify by block number) Fourier Transform Optical Processing		
20. ABSTRACT (Continue on reverse side if necessary and identify by block number) This report describes a device which can take a complete Fourier transform of the intensity transmittance of a photographic transparency. The transform is taken by purely optical means. A complete system analysis is presented, and some results of experiments with the device are described.		

DD FORM 1 JAN 73 1473

EDITION OF 1 NOV 65 IS OBSOLETE

UNCLASSIFIED

SECURITY CLASSIFICATION OF THIS PAGE (When Data Entered)

403 192 LB

1. The first part of the report deals with the general situation of the country and the results of the survey. It is divided into two main sections: a description of the country and a description of the survey. The description of the country is divided into three parts: a general description, a description of the climate, and a description of the population. The description of the survey is divided into two parts: a description of the methods used and a description of the results. The second part of the report deals with the specific results of the survey. It is divided into two main sections: a description of the results of the survey and a description of the conclusions. The description of the results of the survey is divided into three parts: a description of the results of the survey, a description of the results of the survey, and a description of the results of the survey. The description of the conclusions is divided into two parts: a description of the conclusions and a description of the conclusions. The third part of the report deals with the specific results of the survey. It is divided into two main sections: a description of the results of the survey and a description of the conclusions. The description of the results of the survey is divided into three parts: a description of the results of the survey, a description of the results of the survey, and a description of the results of the survey. The description of the conclusions is divided into two parts: a description of the conclusions and a description of the conclusions.

SECURITY CLASSIFICATION OF THIS PAGE(When Data Entered)

PREFACE

This report was done under Project 4A161101A91D. The author would like to acknowledge the support given by his colleagues, John Benton, William Graver, and supervisor Robert Leighty.

COL P. R. Hoge, LTC W. T. Stockhausen, and COL D. L. Lycan were Commanders and Directors of ETL during the study and report preparation. Mr. R. P. Macchia was Technical Director.

Accession For	
NTIS GRA&I	<input checked="checked" type="checkbox"/>
DDC TAB	<input type="checkbox"/>
Unannounced	<input type="checkbox"/>
Justification	
By _____	
Distribution/ _____	
Availability Codes	
Dist	Atail and/or special
A	

CONTENTS

Title	Page
Preface	1
Illustrations	3
Introduction	4
Optical Power Spectrum (OPS) System	4
Effect of Phase Noise	5
Effect of Sampling Aperture	7
The Fourier Transform Autocorrelation (FTA) System	9
Analysis	10
Wave Amplitude Analysis	11
Effect of Piezoelectric Mirror Oscillation	15
Effect of Sampling Aperture on Detector Bandwidth	19
Object Rotation Effects	21
System Position Resolution Requirements	27
Discussion	32

ILLUSTRATIONS

Figure	Title	Page
1	Schematic of a Generalized OPS System	5
2	Fourier Transform Autocorrelation System	11
3	Bessel Functions $J_1(kA)$ and $J_2(kA)$	17
4	FTA System Electronics, Block Diagram	18
5	Physical Interpretation of Double-Valued Output of FTA	24
6	Placing an Aperture on the FTA for Single-Valued Output	26

FOURIER TRANSFORM AUTOCORRELATION

INTRODUCTION

Optical Power Spectrum (OPS) System. ■ The optical Fourier Transform Autocorrelation (FTA) system described in this report was investigated for its ability to overcome two significant problems associated with the usual OPS (Optical Power Spectrum) system. These problems are the presence of phase noise in the object transparency, and the diffraction effects arising from the finite sampling aperture within which the Fourier transform is taken. The essential difference between the conventional OPS system and the FTA system is that the OPS system detects the modulus squared of the Fourier transform of the amplitude transmitted by the object transparency, and the FTA system detects the Fourier transform of the modulus squared of the amplitude (the intensity) transmitted by the object transparency. This report presents an analysis of the FTA system and of the realizations that have been made to implement the theory. Experimental data is lacking because the large amount of data necessary to characterize a transform can only be taken with an automated system.

The study was based on the fact that the Fourier transform of the intensity power transmittance of an object transparency is equal to the autocorrelation of the Fourier transform of the amplitude transmittance of the object transparency. This can be expressed in one dimension as¹

$$F[|\psi(x)|^2] = F[\psi(x)] \otimes F[\psi(x)] \quad (1)$$

where the symbol \otimes denotes correlation, F represents a Fourier transform, and $\psi(x) = A(x) e^{i\phi(x)}$ (where $A(x)$ and $\phi(x)$ are real and $i = \sqrt{-1}$) is the complex amplitude transmittance of the object transparency. Also,

$$\psi(x) \psi^*(x) = |\psi(x)|^2 = A^2(x) \quad (2)$$

is the intensity transmittance of the object transparency. The intensity transmittance is independent of any phase term $\phi(x)$.

¹ R. Bracewell, *The Fourier Transform and Its Applications*, McGraw-Hill, 1965. This book is the reference for all the Fourier transform mathematics used in this report.

The Effect of Phase Noise. ■ In this section, the effect that phase noise and a finite sampling aperture have on the detected signal in an OPS system is described. An OPS system diagram is shown in figure 1.

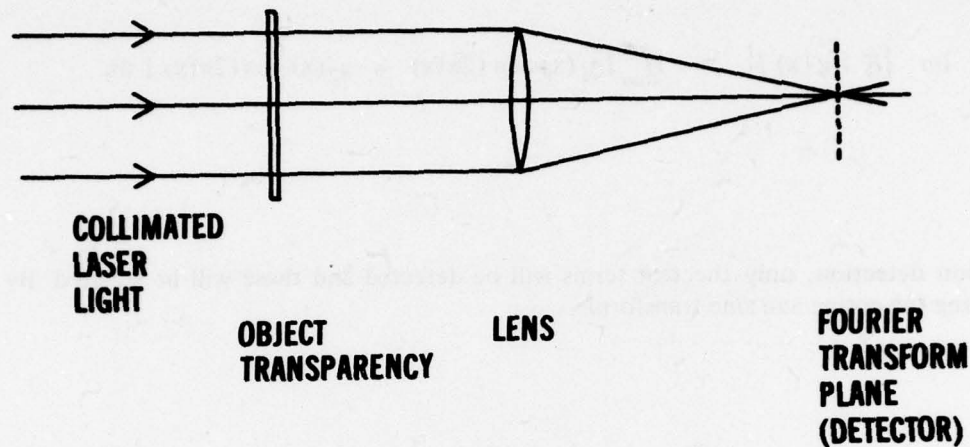


Figure 1. Schematic of a Generalized OPS System.

A squaring detector, such as a photodiode array or photographic film, is used to detect the light energy falling on the transform plane. A squaring detector is a device that senses the energy flow in a radiation field. The name comes from the fact that the energy density is given by the square of the field amplitude. This means, in effect, that if the Fourier transform of the object function $g(x)$ is given by $F[g(x)] = \psi(f)$, then the detected energy is given by $\psi(f) \psi^*(f) = A^2(f)$.

If the object function contains some phase noise terms, then we can define in one dimension.

$$g(x) = g_1(x) + ig_2(x) \quad (g_1(x) \text{ and } g_2(x) \text{ real}) \quad (3)$$

where $g_1(x)$ represents the amplitude transmittance of the transparency resulting from the silver grain image on it and $g_2(x)$ represents the phase noise caused by emulsion surface relief and index of refraction inhomogeneities in the emulsion and film base.

Fourier transforming $g(x)$ and separating the real and imaginary parts of the transform yields

$$\operatorname{Re} \{F[g(x)]\} = \int_{-\infty}^{\infty} [g_1(x) \cos(2\pi fx) + g_2(x) \sin(2\pi fx)] dx \quad (4)$$

$$\operatorname{Im} \{F[g(x)]\} = i \int_{-\infty}^{\infty} [g_1(x) \sin(2\pi fx) + g_2(x) \cos(2\pi fx)] dx \quad (5)$$

Upon detection, only the real terms will be detected and these will be squared. By defining the cosine and sine transforms,

$$C[g_1(x)] = \int_{-\infty}^{\infty} g_1(x) \cos(2\pi fx) dx \quad (6)$$

$$S[g_2(x)] = \int_{-\infty}^{\infty} g_2(x) \sin(2\pi fx) dx \quad (7)$$

Then, detection will give

$$|\operatorname{Re} \{F[g(x)]\}|^2 = C^2[g_1(x)] + S^2[g_2(x)] + 2 C[g_1(x)] S[g_2(x)] \quad (8)$$

Expressing equation 8 in words; the odd components of the phase noise $g_2(x)$ will be transformed into an amplitude distribution, which will be added to the even components of the amplitude due to $g_1(x)$ and will be mixed with the desired signal from $g_1(x)$ when the Fourier transform is detected. Equation 8 shows that phase noise is a serious problem in pattern recognition because it obscures the desired information due to $g_1(x)$ in the detected OPS.

The Effect of the Sampling Aperture. ■ The aperture used to define the area of a photograph that is sampled and transformed is also a source of noise. The limited region of $g(x)$ means that the Fourier transform is no longer evaluated over all space, but rather only between some finite limits x_1 and x_2 . This limitation causes the transform of $g(x)$ to be convolved with the transform of the aperture function. This aperture function is defined somewhat artificially, so that we may still have a Fourier transform integral from $-\infty$ to ∞ . Let the aperture function be defined as centered on $x = 0$, so that

$$x_1 = -x_2 = d.$$

$$\text{aperture} = \text{rect} \left(\frac{x}{2d} \right) \equiv \begin{cases} 1 & \text{for } |x| < d \\ 0 & \text{for } |x| > d \end{cases} \quad (9)$$

and the transform

$$\int_{-d}^d g(x) e^{-i2\pi f x} dx \equiv \int_{-\infty}^{\infty} \text{rect} \left(\frac{x}{2d} \right) g(x) e^{-i2\pi f x} dx \quad (10)$$

Now, we can make use of the fact that

$$F \left[\text{rect} \left(\frac{x}{2d} \right) \right] = 2d \text{sinc}(2df) \quad (11)$$

where

$$\text{sinc}(x) = \frac{\sin(\pi x)}{\pi x} \quad (12)$$

and the theorem that for any two functions $a(x)$ and $b(x)$

$$F [a(x) b(x)] = F [a(x)] * F [b(x)] \quad (13)$$

where the asterisk denotes convolution.

The final result is

$$\int_{-\infty}^{\infty} \text{rect} \left(\frac{x}{2d} \right) g(x) e^{-i2\pi fx} dx = 2d \text{sinc}(2df) * F [g(x)] \quad (14)$$

In an OPS system, the convolved amplitudes are squared, which effectively prevents the removal of the aperture effect from the detected signal. In general, deconvolution can not be performed without retransforming the complete complex signal into a multiplication problem, after which the aperture function can be divided out. However, deconvolution is an excessively difficult and noisy operation and is not done in practice. The effect of the aperture function is most evident at the "d.c. spike" of the transform caused by the average or zero spatial frequency which contains most of the energy in the transform. The transformed aperture function around the d.c. spike is removed by subtracting the amplitude field owing to the aperture. However, if the amplitude field is squared, then the aperture effect is multiplied with the desired signal and cannot be removed by subtraction. Because the aperture function cannot be deconvolved or even subtracted in the zero order, much effort has been spent on apodization, defined as rolling off the aperture transmittance as a function of radius to prevent ringing of the aperture transform. Unfortunately, apodization also removes the important property of translation invariance from the detected transform modulus and severely restricts the usefulness of the OPS system as a pattern recognition device.

The Fourier Transform Autocorrelation System. • Figure 2 is a diagram of the FTA system designed to implement equation 1. The system is essentially a Twyman-Green interferometer, whose mirror plane is imaged by a telescope into the object plane. Light transmitted through the object plane is then collected and detected by a photomultiplier tube (PMT) detector. The two beams of the interferometer, one from each arm, give two transforms $F [g(x)]$, and an angle between the beams gives the correlation to synthesize the function

$$F [g(x)] * F [g(x)]$$

as in equation 1.

The title "Fourier Transform Autocorrelation" is somewhat misleading because, even though the original idea for this system came from equation 1, it has been found to be more fruitful to analyze the FTA system as a detector of moiré patterns formed between a projected cosine grating generated by the interferometer and similar spatial frequencies in the object transparency. Complicated objects, such as an aerial photograph, contain many spatial frequencies and directions in which these spatial frequencies are found. The determination of the amplitudes, phases, and directions of these spatial frequencies constitutes taking the Fourier transform of the object transparency. The analysis section that follows will show how the FTA device takes a Fourier transform and will discuss details of implementation.

ANALYSIS

The analyses contained in this section are briefly described below (All of the descriptions refer to figure 2). The analysis proceeds from the most general and mathematically simplest form into more detailed considerations dictated by the particular apparatus used. Analyses 1 and 2 are concerned with the heterodyne methods that have been tried. Analyses 3 and 4 determine the system spread function, (therefore its resolution), and analysis 5 is concerned with system tolerances and mechanical requirements.

Analysis 1: Wave Amplitude Analysis is a description of the case where mirror M1 is tilted through an angle θ , and mirror M2 is linearly translated in a direction normal to its surface at a constant velocity v .

Analysis 2: Effect of Piezoelectric Mirror Oscillation shows the effect of oscillating mirror M2 sinusoidally rather than translating it with constant velocity. This method has great advantages in experimental simplicity and in ease of analysis of the detected signal.

Analysis 3: Effect of Sampling Aperture on Detector Bandwidth shows the effect of the system aperture on the bandwidth of spatial frequency detection in the Fourier transform plane. This in effect defines the system point spread function in the spatial frequency or radial direction in the transform space.

Analysis 4: Object Rotation Effects shows the effect of object rotation on signal detection. In effect, this defines the system point spread function in angle (α) in transform space. Together with analysis 3, we then have a theoretical point spread function for the system.

Analysis 5: System Position Resolution Requirements is an analysis of the resolution needed in the tilting of mirror M1 and in the rotation of the object such that a Fourier transform resolution consistent with the device spread function may be obtained.

Wave Amplitude Analysis. ■ The FTA device initially operated by tilting mirror M1 through angle θ . Mirror M2 remained normal to the beam but was linearly translated along the optical axis at a velocity v . The object transparency was located in the object plane of figure 2. Angle θ lies in the plane of the interferometer, which will be called the x, z plane. Thus, z is defined to be along the path of the light, x is positive upward in figure 2, and y is positive out of the paper in order that x, y, z may form a right-handed coordinate system. Since the telescope is a 1:1 system, an angle θ at mirror M1 will be imaged into the same angle θ in the object plane. Mirror M1 is imaged into the object plane by the telescope, as shown in dashed lines, so that a tilt θ does not result in a beam translation in the object plane. The two plane wave beams from M1 and M2 give the following normalized amplitudes:

$$M1: e^{-ik\theta x} \quad \text{where } k = \frac{2\pi}{\lambda} \text{ and } \lambda = \text{wavelength of light (632.8nm)}$$

$$M2: e^{ikvt} \quad \text{where } v = \text{velocity of mirror in direction of light path}$$

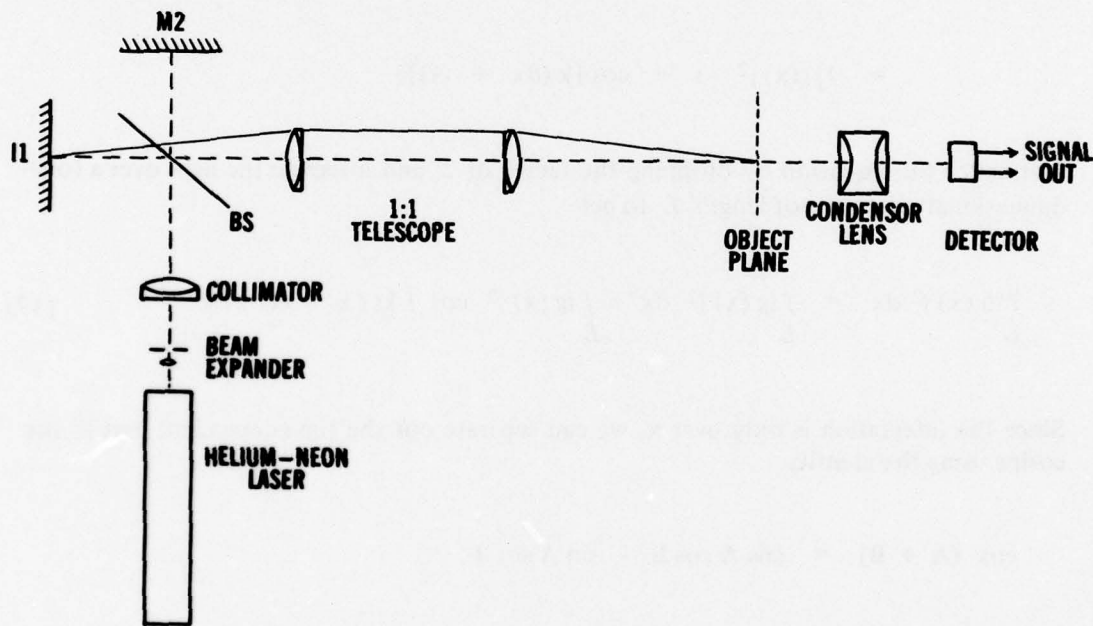


Figure 2. Fourier Transform Autocorrelation System.

The sum of these two beams produces the amplitude field incident on the object plane. This field is multiplied by the object transmission function $g(x,y)$ to produce the amplitude field just behind the object plane. Because the system only reads out along the x -axis, we reduce the amplitude field equation to one dimension:

$$h(x) = [e^{ikvt} + e^{-ik\theta x}] g(x) \quad (15)$$

This field is detected (integrated) by a squaring detector to give

$$\begin{aligned} h(x) h^*(x) &= |h(x)|^2 \\ |h(x)|^2 &= [e^{ikvt} + e^{-ik\theta x}] g(x) [e^{-ikvt} + e^{ik\theta x}] g^*(x) \\ &= |g(x)|^2 [2 + e^{-ik(\theta x + vt)} + e^{ik(\theta x + vt)}] \\ &= 2|g(x)|^2 \{1 + \cos[k(\theta x + vt)]\} \end{aligned} \quad (16)$$

Normalize this equation by dropping the factor of 2, and integrate the light over a (one-dimensional) detector of length L to get

$$\int_L |h(x)|^2 dx = \int_L |g(x)|^2 dx + \int_L |g(x)|^2 \cos[k(\theta x + vt)] dx \quad (17)$$

Since the integration is only over x , we can separate out the time-dependent part of the cosine using the identity

$$\cos(A + B) = \cos A \cos B - \sin A \sin B$$

$$\begin{aligned} \int_L |h(x)|^2 dx &= \int_L |g(x)|^2 dx + \cos(kvt) \int_L |g(x)|^2 \cos(k\theta x) dx \\ &\quad - \sin(kvt) \int_L |g(x)|^2 \sin(k\theta x) dx \end{aligned} \quad (18)$$

The two forms, equation 17 and 18 show different properties of the result.

Equation 17 has the important second integral in the form of a correlation of $g(x)^2$ with $\cos(k\theta x)$. The definition of correlation is

$$g \otimes h = \int_{-\infty}^{\infty} g(u) h(u + x) du \quad (19)$$

To give the response of a finite system, the correlation must be multiplied by the system aperture L . This action does not invalidate the correlation, but only causes convolution of the result by a spread function characteristic of the aperture (see analysis 3).

Equation 18 shows that for a given spatial frequency $\cos(k\theta x)$ there are two detectable time-varying terms which appear in quadrature. If we can obtain a reference signal of the same temporal frequency as $\cos(kvt)$, we can separate the last two integrals of equation 16 by phase detection. This separation is very important since the form of these two integrals is that of a cosine transform and a sine transform of $|g(x)|^2$. If we can separate these two integrals in the readout, we can then obtain the complete Fourier transform of $|g(x)|^2$ from the identity.

$$F[h(x)] = C[E(x)] + i S[O(x)] \quad (20)$$

where C = cosine transform

S = sine transform

$E(x)$ = even part of $h(x)$

$O(x)$ = odd part of $h(x)$

If the function $h(x)$ is completely real, as $|g(x)|^2$ is, then its even part transforms to a real function, and its odd part transforms to an imaginary function. Therefore, the even and odd parts do not need to be separated, since the sine and cosine transforms will do that for us. We then get the simplified result

$$F[|g(x)|^2] = C[|g(x)|^2] + i S[|g(x)|^2] \quad (21)$$

which is a combination of the last two integrals of equation 18. To examine the effect of having the complete Fourier transform of $|g(x)|^2$, define the apertured amplitude function in the input plane as

$$g(x) = \text{rect}\left(\frac{x}{D}\right) [A + g_r(x) + i g_i(x)] \quad (22)$$

where we have split $g(x)$ into its average amplitude A , its real varying part $g_r(x)$, and its imaginary varying part $g_i(x)$.

$$\begin{aligned} |g(x)|^2 &= \text{rect}^2\left(\frac{x}{D}\right) [A + g_r(x) + i g_i(x)] [A + g_r(x) - i g_i(x)] \\ &= \text{rect}^2\left(\frac{x}{D}\right) [A^2 + g_r^2(x) + g_i^2(x) + 2A g_r(x)] \end{aligned} \quad (23)$$

Now use the fact that $\text{rect}^2\left(\frac{x}{D}\right) = \text{rect}\left(\frac{x}{D}\right)$, and transform

$$\begin{aligned} F[|g(x)|^2] &= D \text{sinc}(Df) * \{A^2 \delta(f) + F[g_r^2(x)] + F[g_i^2(x)] + 2AF[g_r(x)]\} \\ &= D \text{sinc}(Df) * \{A^2 \delta(f) + F[|g(x)|^2] + 2AF[g_r(x)]\} \end{aligned} \quad (24)$$

The FTA apparatus gives this Fourier transform, and the term $A^2 D \text{sinc}(Df)$, centered at $f = 0$, can be digitally subtracted. This process removes the effect of the aperture convolved with the d.c. spike in the transform. Although this is not equivalent to deconvolving the aperture function at all points of the transform, it does remove the most troublesome aperture effect which is troublesome because of the extreme intensity of the d.c. term. As stated earlier, this is done without apodization, and the position invariance property of the transform modulus is retained.

Effect of Piezoelectric Mirror Oscillation. ■ This method was investigated because of experience with a system incorporating the idea presented in analysis 1; where the mirror M2 was translated at a constant velocity v over a long distance. This translation was accomplished by moving a stage with a 1-inch micrometer, driven by a synchronous 60-RPM motor. Mirror M2 was mounted atop the stage. A switch mechanism reversed the motor at the end of its travel in each direction, and data was taken in the middle of travel. Two problems were evident with this system. First, the stage did not have straight ways, and a progressive tilt was introduced into the beam as the stage moved away from the center of its range where it had been initially adjusted. Second, the synchronous motor did not give a constant velocity because of an inherent property of such motors called "cogging." The only way to eliminate cogging is by using a flywheel, which would be difficult to fit and would hamper reversing. These problems prompted the following analysis in which mirror M2 is oscillated by a piezoelectric (PZ) driver rather than linearly translated by a micrometer-driven stage.² A diagram of the electronics required for PZ modulation of the FTA is shown in figure 4.

In equation 15 replace $(v t)$ with

$$A \sin (2\pi f t) = A \sin (\omega t)$$

where: A = amplitude of oscillation of PZ

f = frequency of oscillation of PZ

$\omega = 2\pi f$ = phase velocity

Then, by a similar analysis, we get the detected signal

$$\begin{aligned} \int_L |h(x)|^2 dx &= \int_L |g(x)|^2 dx + \cos[kA \sin(\omega t)] \int_L |g(x)|^2 \cos(k\theta x) dx \\ &\quad - \sin[kA \sin(\omega t)] \int_L |g(x)|^2 \sin(k\theta x) dx \end{aligned} \quad (25)$$

²This idea was developed from lectures in Geometrical Optics by Duncan Moore at the Institute of Optics of the University of Rochester, NY.

The amplitudes of the cosine and sine transforms can be expressed as Bessel series expansions using the following identities:

$$\cos [kA \sin (\omega t)] = J_0(kA) + 2J_2(kA) \cos (2\omega t) + 2J_4(kA) \cos (4\omega t) + \dots$$

$$\sin [kA \sin (\omega t)] = 2J_1(kA) \sin (\omega t) + 2J_3(kA) \sin (3\omega t) + 2J_5(kA) \sin (5\omega t) + \dots$$

This is a very useful result because we see that simple frequency bandpass filtering will give the coefficients of the sine and cosine transforms without a phase reference signal or phase detection systems. More precisely, if we detect the fundamental frequency (ωt), then for a constant amplitude of PZ oscillation,

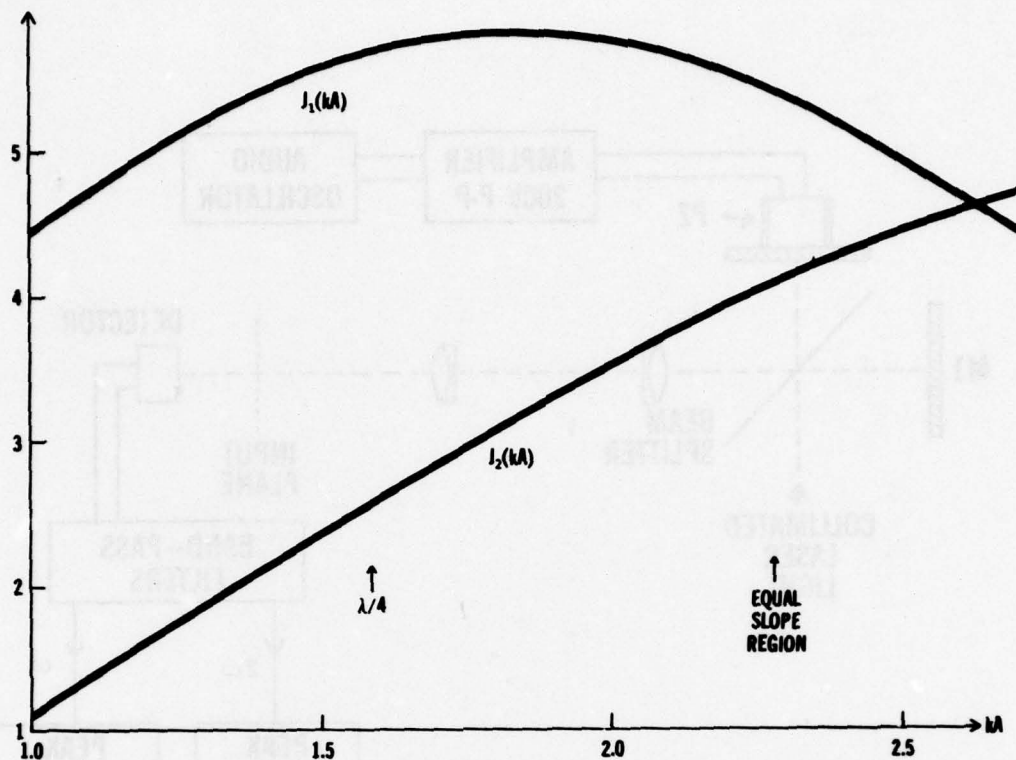
$$\frac{\text{detected amplitude}}{2J_1(kA)} = M \quad (26)$$

Detection of the first harmonic ($2\omega t$) frequency then gives

$$\frac{\text{detected amplitude}}{2J_2(kA)} = N \quad (27)$$

where M and N are the amplitudes of the sine and cosine transforms respectively, of the particular spatial frequency of $|g(x)|^2$ which is being tested for as determined by the mirror angle θ . The value of $J_1(kA)$ and $J_2(kA)$ must be accurately known to get a good result. It is useful to plot $J_1(kA)$ and $J_2(kA)$ to find the region of kA that will give the best result. For $kA > 3$, the J_1 and J_2 functions are approximately in quadrature; so it is useful to consider the region $1 < kA < 3$, which encompasses amplitudes of slightly less than $\frac{1}{4}\lambda$ to around $\frac{1}{2}\lambda$ at which $kA = \pi$. The graph shows that the region about halfway between $\frac{1}{4}\lambda$ and $\frac{1}{2}\lambda$ gives the best combination of high amplitude and low slope for the functions (figure 3). Low slope is desirable so that the value of the function is not too sensitive to slight amplitude changes of the PZ driver.

Without using electronic phase detection it is difficult to get an accurate value for the optical path difference ($OPD = kA$). Without an accurate OPD it is impossible to calculate accurate values of $J_1(kA)$ and $J_2(kA)$ and, thereby to get good values for the amplitudes of the sine and cosine transforms.



The principal problem associated with OPD detection is that the origin of coordinates for the sinusoidal fringe pattern projected by the interferometer is unknown. This leads to a phase ambiguity that is not constant for different spatial frequencies. If the modulus of $F [|g(x)|^2]$ is required, this phase ambiguity does not have to be recovered; but if the complete transform is needed (as it is for such operations as deconvolution of aperture effects), then a phase reference must be provided. A reference phase can be derived at low spatial frequencies by sampling a portion of the field input to the object transparency. This could be done with a beamsplitter, a microscope objective to magnify the fringes, and a detector to sample the field in a small region. Although high spatial frequencies cannot be phase-referenced by the method described, it is only necessary to know the phase of low spatial frequencies (up to about 10 cycles per millimeter) for the purpose of deconvolution of an aperture function. The problem of aperture function deconvolution will be addressed in the next section of this report.

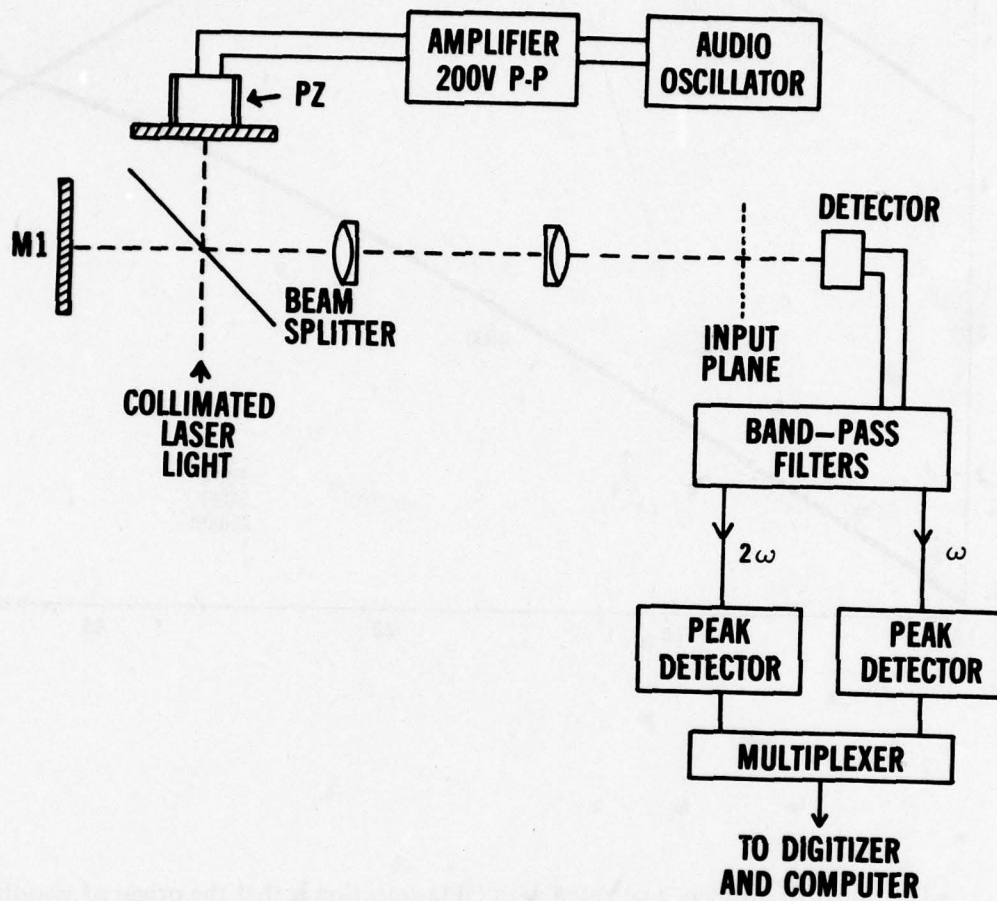


Figure 4. FTA System Electronics Block Diagram.

Effect of Sampling Aperture on Detector Bandwidth. ■ The detected moire pattern, will cause a signal amplitude in the detector which is proportional to the original moire fringe contrast, fringe spacing, and system aperture. The system aperture is the sampling aperture on the object and will be circular. Let the moire pattern equation be

$$I = I_0 [1 + m \cos (2\pi f x)]$$

$m =$ contrast

$f =$ spatial frequency in x-direction

(28)

Normalize the intensity by $I_0 = 1$ and integrate this function over a circular aperture of radius $\ell/2$ using polar coordinates r, θ where $x = r \cos \theta$.³

$$I = 2 \int_0^\pi \int_0^{\ell/2} [1 + m \cos (2\pi f x)] r dr d\theta$$

$$= 2 \int_0^\pi \int_0^{\ell/2} r dr d\theta + 2 m \int_0^\pi \int_0^{\ell/2} \cos (2\pi f r \cos \theta + 2\pi f x_0) r dr d\theta$$
(29)

The arbitrary phase shift $2\pi f x_0$ has been added to make the result general. The first integral is just twice the detector area. Split the second integral into two integrals by

$$\cos (A + B) = \cos A \cos B - \sin A \sin B$$

The resulting integrals must be evaluated from tables, but the final result for the detected signal is

$$\text{output} = (\text{constant}) [1 + m \left(\frac{2J_1(\pi \ell f)}{\pi \ell f} \right) \cos(2\pi f x_0)]$$
(30)

The observed fringe contrast is now $m \left(\frac{2J_1(\pi \ell f)}{\pi \ell f} \right)$ rather than just m , which shows that as the aperture is made larger, the Δf range over which a good response is seen is reduced. The effect is that the instrument spread function in the synthesized Fourier transform space is a Besinc function, just as it is for conventional optical Fourier transforms using circular apertures.

³This section developed from lectures in Interferometry by M. Parker Givens at the Institute of Optics of the University of Rochester, NY.

Since we are dealing with a Besinc function, Rayleigh's criterion may be used for resolvable points in the transform plane. This criterion is defined as the distance in frequency space from the central maximum of the Besinc function to its first zero. The first zero of the function is at 1.220π . Substituting the argument of our derived function, we get

$$\pi \ell f = 1.220\pi$$

$$\Delta f = \frac{1.220}{\ell}$$

The following table was generated using Rayleigh's criterion:

<u>aperture diameter (ℓ) in mm</u>	<u>$\pm \Delta f$ in cycles/mm</u>
1	± 1.22
2	± 0.61
3	± 0.41
4	± 0.31
5	± 0.24
6	± 0.20
7	± 0.17
8	± 0.15
9	± 0.14
10	± 0.12

This table indicates the extreme sensitivity of the system. The narrow spread function means that the tilt of mirror M1 to scan in frequency must be very precise, and the rotation of the object transparency to scan in direction α must be similarly precise. An exact calculation of these requirements is in Analysis 5.

Object Rotation Analysis. ■ For the purpose of this analysis, assume that the sampling aperture of the FTA is infinite. This assumption is equivalent to saying that the device point-spread function (psf) will be a delta function. To find the psf of a real device with a finite sampling aperture, we only have to convolve the psf found in this analysis with the Fourier transform of the sampling aperture. In the previous section this function was shown to be a Besinc for circular apertures.

The assumption of an infinite sampling aperture simplifies this analysis and enables the result to be more general. The detector acts as a low-pass spatial frequency device that will only pass a zero spatial frequency moiré for an infinite sampling aperture. This low-pass filtering means that the difference frequency between the cosine grating projected by the interferometer and some spatial frequency in the object must be zero to be detected. To derive the conditions under which this difference spatial frequency is zero, assume an object function consisting of a single spatial frequency in the x direction. The field immediately behind the object transparency is then given in normalized form by

$$\psi(x) = [1 + A \cos(2\pi f_1 x)] \cos(2\pi f_2 x + \gamma) \quad (31)$$

where

A = transparency modulation as a fraction of average transmittance

f_1 = object spatial frequency

f_2 = spatial frequency projected onto object

γ = arbitrary phase offset

For simplicity in notation, define

$$P = 2\pi f_1 x$$

$$Q = 2\pi f_2 x$$

The optical field is then rewritten as

$$\begin{aligned}\psi(x) &= [1 + A \cos(P)] \cos(Q + \gamma) \\ &= \cos(Q + \gamma) + A \cos(P) \cos(Q + \gamma)\end{aligned}\tag{32}$$

Detection of this field then gives (33)

$$|\psi(x)|^2 = \cos^2(Q + \gamma) + 2A \cos(P) \cos^2(Q + \gamma) + A^2 \cos^2(P) \cos^2(Q + \gamma)$$

Since it must collect all the light passing through the FTA device, the detector must also be infinite in extent. This requirement is of course relaxed for a real device with a finite sampling aperture. Use trigonometric identities to remove squared cosines, and get the following equation whose terms are grouped into significant categories:

$$\begin{aligned}|\psi(x)|^2 &= 1/2 + A^2/4 && \text{bias terms} \\ &+ 1/2 \cos(2Q + 2\gamma) + A \cos(P) && \text{high-frequency terms} \\ &+ (A^2/4) \cos(2Q + 2\gamma) + (A/4) \cos(2P) \\ &+ A \cos(P) \cos(2Q + 2\gamma) && \text{cross terms} \\ &+ (A^2/4) \cos(2P) \cos(2Q + 2\gamma)\end{aligned}\tag{34}$$

The detector acts as a low-pass filter for spatial frequencies so that the high frequency terms will not be detected. To determine detectability of the cross terms, expand them by trigonometric identities.

$$\begin{aligned}A \cos(P) \cos(2Q + 2\gamma) &= (A/2) \cos(P - 2Q - 2\gamma) + (A/2) \cos(P + 2Q + 2\gamma) \\ (A^2/4) \cos(2P) \cos(2Q + 2\gamma) &= (A^2/8) \cos(2P - 2Q - 2\gamma) + (A^2/8) \cos(2P + 2Q + 2\gamma)\end{aligned}\tag{35}$$

(36)

Low-pass filtering will not detect the sum terms. The detectable terms are now reduced to a manageable size. Substituting back for P and Q, we get the detectable terms

$$\begin{aligned}
 |\psi(x)|_{\text{filtered}}^2 &= \frac{2 + A^2}{4} + (A/2) \cos [2\pi x (f_1 - 2f_2) - 2\gamma] \\
 &+ (A^2/8) \cos [4\pi x (f_1 - f_2) - 2\gamma]
 \end{aligned}
 \tag{37}$$

Assuming an infinite sampling aperture, the cosine terms will be detected when

$$f_1 - 2f_2 = 0$$

and

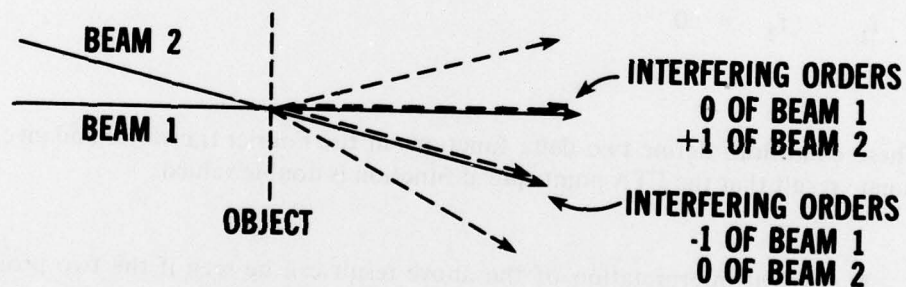
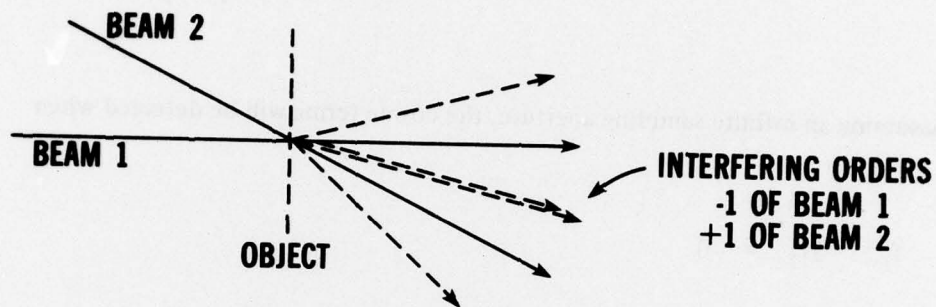
$$f_1 - f_2 = 0$$

These conditions define two delta functions in the Fourier transform and give the unfortunate result that the FTA point-spread function is double valued.

A physical interpretation of the above result can be seen if the two projected light beams are diffracted into plus and minus orders by an object function consisting of a biased cosine grating, which gives the two coincidence conditions as shown in Figure 5.

a) condition $f_1 - 2f_2 = 0$ where f_1 = object spatial frequency

f_2 = projected grating spatial frequency



Note that beam 1 is fixed and beam 2 is steered.

Figure 5. Physical Interpretation of Double-Valued Output of FTA.

Notice that the condition $f_1 - 2f_2 = 0$ appears as interference along a single direction and the condition $f_1 - f_2 = 0$ appears as interference along two directions. The influence of the fundamental term ($f_1 - f_2 = 0$) drops as the modulation of the object grating decreases as can be seen from the table below.

<u>A</u>	<u>A/2</u>	<u>A²/8</u>	<u>A²/8 as % of A/2</u>
1	0.5	0.125	25
0.5	0.25	0.031	13
0.3	0.15	0.011	7
0.1	0.05	0.0013	3
0.05	0.025	0.00031	1.3

The variable A is the object modulation, A/2 is the coefficient of the first harmonic term ($f_1 - 2f_2 = 0$) and A²/8 is the coefficient of the fundamental harmonic term.

An attempt to change the FTA from a double-value to a single-valued device would necessitate Fourier transforming the output and aperturing in the detector space to block out unwanted orders. Examination of figure 5 shows that the -1 order of beam 1 takes part in both condition (a) and one of the beams of condition (b). Detection of an unambiguous frequency requires an attempt to isolate the beam corresponding to the zero order of beam 1 and the +1 order of beam 2 as shown in condition (b). Isolation of this desired beam is made easier by the fact that beam 1 is fixed in direction so the aperture need not be moved as the device scans in spatial frequency. Other considerations mitigate against such a solution however. First, the time-varying amplitude of the isolated beam will have a coefficient of A²/16 and will give signal-to-noise problems at the low modulations found in aerial photography. Second, the zero order of beam 1 is very strong (bright) and will cause a large bias term leading to an increase in detector noise. These two considerations are very important because bench work has shown that the FTA device has a signal-to-noise problem that is quite severe.

If it is desirable to attempt to aperture the output of the FTA device as described above, a criterion for minimum detectable spatial frequency can be derived. This criterion will necessarily be dependent on the size of the sampling aperture used in the object plane because readings of spatial frequency will be degraded by energy from unwanted

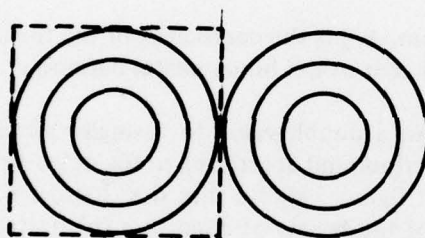
diffraction orders entering the detector aperture. This energy comes from ringing of the transform of the input aperture function. As an example of such calculation, note that the Besinc function has the normalized form given in the preceding section.

$$\frac{2J_1(\pi \ell f)}{(\pi \ell f)}$$

where ℓ = diameter of object plane aperture

f = spatial frequency

If we want to collect energy from this "spread function" out to the third zero-crossing without collecting energy beyond the third zero-crossing of the adjacent (and unwanted) order, we have the situation shown in figure 6.



Zeros of Besinc functions are indicated by circles, the sampling aperture is indicated by a dashed line.

Figure 6. Placing an Aperture on the FTA For Single-Valued Output.

From tables, the third zero of the Besinc function is found when the argument is 10.173, that is

$$\pi \ell f = 10.173$$

The orders are separated by twice this distance; so the solution for minimum detectable spatial frequency is

$$f = \frac{20.35}{\pi \ell}$$

which can be seen to be inversely related to the object sampling aperture size. Some representative values are

<u>ℓ (mm)</u>	<u>f (cy/mm)</u>
10	0.65
5	1.30
1	6.48

Notice that the optimum size of the detector aperture is also dependent on the object sampling aperture diameter. Criteria for any separation of desired and unwanted orders can be similarly derived.

System Position Resolution Requirements. ■ To realize the potential device resolution given by Rayleigh's criterion, mechanical rigidity and high positional accuracy of the tilt (θ) of mirror M1 (figure 2) and the rotation (ϕ) of the object transparency in its own plane will be required. The analysis in this section will provide some numbers to be used in apparatus design. Assume that the maximum sampling aperture to be used in the system will be 10 millimeters in diameter, that the maximum spatial frequency of interest is 100 cycles per millimeter, and that the telescope in the device images at 1:1.

A maximum aperture of 10 millimeters implies by Rayleigh's criterion that the frequency spread $\Delta f = \pm 0.122$ cycle per millimeter. This then corresponds to the necessity of setting the angle of mirror M2 to a $\Delta\theta$ given by differentiating the grating equation for normal incidence.

$$\sin \theta = f \lambda \text{ where } f = \frac{1}{\text{grating spacing}}$$

$$\frac{d(\sin \theta)}{df} = \lambda \quad (38)$$

$$\frac{\cos \theta d\theta}{df} = \lambda$$

$$d\theta = \frac{\lambda df}{\cos \theta}$$

$$d\theta = \frac{0.6328 \times 10^{-3}}{0.122} \text{ mm} \quad (39)$$

$$d\theta = 7.7202 \times 10^{-5} \text{ radian}$$

$$\approx 16 \text{ arc seconds}$$

Using a micrometer that can be read to 0.001 inch, we need a pivot arm on mirror M1 of a length given by

$$d\theta \text{ (radians)} = \frac{.001}{x}$$

$$x = \frac{.001}{7.7202 \times 10^{-5}} = 12.95 \text{ inches}$$

This will give a $\Delta\theta$ least count consistent with Rayleigh's criterion. Using a micrometer with a total travel of 1 inch will give a maximum angle of about 4° , and since 3.63° corresponds to a grating frequency of 100 cycles per millimeter this will be a good choice.

A standard micrometer screw has 40 turns per inch. If the micrometer is turned by a 60 revolutions per minute motor, then a sample must be taken every 0.04 second, which implies that 40 cycles of a 1,000 Hertz modulation frequency will be sampled in each interval. This should give a good P-P signal value. The bandwidth of the filter circuits that isolate signals on the output of the PMT will then be

$$BW = \frac{1}{2\tau} = \frac{1}{2(1/25)} = 12.5 \text{ Hz} \quad (40)$$

This should give good noise rejection.

A scan at one angular orientation of the object transparency will take 33 turns, or 33 seconds, to go from 0 to 100 cycles per millimeter in spatial frequency. Allowing a turn-around time, it is reasonable to assign 40 seconds to a single radial scan in spatial frequency.

In addition to scanning in spatial frequency, the device must scan in angle ϕ in order to read out the two-dimensional Fourier transform of the object. Because of the symmetry of the modulus of the Fourier transform of a real object, only a scan over an angle $\phi = 180^\circ$ need be taken if the modulus of the transform is of interest. To calculate the increment Δx needed to satisfy Rayleigh's criterion, notice that the number of radial samples just calculated is given by

$$\frac{100 \text{ cycles/mm}}{0.122 \text{ cycles/mm}} = 820 \text{ samples}$$

Then, around the circumference of the transform plane from 0 to 180° we have

$$820\pi \approx 2580 \text{ resolvable } \Delta\phi \text{ samples}$$

then,

$$\Delta\phi = \frac{180^\circ}{2580} = 0.0698^\circ = 4'11''$$

The total number of data points will be

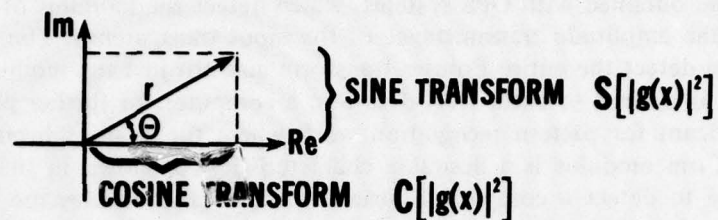
$$\frac{\pi}{2} (820)^2 = 1,056,203$$

and the total time required will be

$$40 \text{ seconds} \times 2580 = 103,200 \text{ seconds}$$

$$= 29 \text{ hours}$$

By using a small sampling aperture, the number of sample points will be reduced in proportion to its area. Although it might be possible to go to faster data sampling rates, this system has a signal-to-noise ratio problem; therefore, a conservative design is desirable. Implementating a spiral scan through the transform space may enable data to be collected more efficiently by eliminating the redundancy at low spatial frequencies, which the radial scan provides. Radial scanning is assumed in this design for experimental simplicity. Current plans for data handling are to plot sine and cosine transforms on an analog plotter. In a later generation device, these transforms can be digitized and the Fourier transform phase and modulus can be calculated using the mathematical equivalent of an Argand diagram. An Argand diagram is shown on the next page.



mathematically, by trigonometry we get

$$\begin{aligned}
 F [|g(x)|^2] &= r e^{i\theta} \\
 &= (S^2 [|g(x)|^2] + C^2 [|g(x)|^2])^{1/2} \exp \left\{ i \tan^{-1} \left(\frac{S [|g(x)|^2]}{C [|g(x)|^2]} \right) \right\}
 \end{aligned}
 \tag{41}$$

The resulting values of modulus and phase can be stored for later processing or display.

DISCUSSION

The FTA device is unique in its capability to take a complete Fourier transform (amplitude and phase) of the intensity transmittance of an input transparency by purely optical means. This capability is valuable because of the deleterious effect of phase noise on readings obtained with OPS systems, which detect the modulus of the Fourier transform of the amplitude transmittance of the input transparency. The fact that the FTA device can detect the entire Fourier transform and not just the modulus, may be significant if it is desired to enter FTA data into a computer for further processing, but it is not significant for pattern recognition work where the position-invariance property of the transform modulus is a desirable characteristic. As shown in the Analysis section, the ability to detect a complete Fourier transform also enables the subtraction of the transform of the sampling aperture that is convolved with the d.c. spike in the transform plane. This capability can be useful for those cases where measurements of low spatial frequency components are impeded by the ringing of the sampling aperture transform.

Although it has the above stated advantages, the FTA has inherent disadvantages, which cause problems that do not have solutions at this time.

Briefly, these problems are:

1. The FTA is not a parallel processor in that the Fourier transform of the input must be built up one point at a time.
2. Data rates are slow. This can be improved somewhat by engineering, but will remain a problem because of the mechanical motions that are required.
3. The device output is double valued. Aperturing in the transform plane can eliminate this problem at a cost of signal-to-noise ratio as shown in the Object Rotation Effects section.
4. The signal-to-noise ratio is poor because of the large background bias that is always present.
5. Extremely precise mechanical movements are required for reasonable sampling conditions as shown in the preceding section. This requires a great deal of stability in the apparatus.

In bench work with a prototype, problems 4 and 5 were found to be very severe. Although this is to be expected from new experiments, the degree of rigidity and precision required to make repeatable readings would necessitate extreme measures in a final device design.

This study has been terminated because of the problems listed above. The insights into the details of Fourier transformation by optical systems that have been gained in this study have been applied in other projects at ETL. In particular, a deeper appreciation of the problem of phase noise in OPS systems has been achieved that will lead to other less cumbersome methods for eliminating this noise from measurements taken with OPS systems. A significant reduction or elimination of phase noise should lead to a much more valuable pattern classifier that is capable of a wider range of classification than is possible with current systems.